Smoke Characteristics of Tunnel Wood Fires

Calvin K. Lee, Joseph M. Singer and Kenneth L. Cashdollar
Pittsburgh Mining and Safety Research Center, Bureau of Mines, US Department of Interior, 4800 Forbes Avenue, Pittsburgh, Pennsylvania 15213, USA.

Characteristics of smoke particulates generated from a wood fire in a ventilated model tunnel were investigated using an *in situ* optical and a grid sampling technique. Volume-to-surface mean diameter and mass concentration of the smoke particles, and the transmission, optical density per unit length and particulate optical density of the smokeladen exhaust gas were obtained as a function of the burning process in the tunnel. It was found that high concentrations of smoke (~ 1 mg l^{-1}) were rapidly generated as the fire changed from oxygen-rich to fuel-rich burning, resulting in fast obscuration of the passageway. The simultaneous generation of large amounts of smoke and high temperature carbon monoxide ($\sim 8\%$) coupled with the low transmission ($\sim 1\%$ through 0.5 m) represents an extremely hazardous situation in such a fire environment. Present measurements and others from current smoke testing chambers are compared and discussed.

INTRODUCTION

The physiological hazard of smoke particulates in fires has prompted recent theoretical and experimental investigations of the smoke characteristics of natural and synthetic fuels. Among these studies, Seader *et al.*[1–3] have made advances in the understanding of the effect of smoke properties on optical obscuration and in the correlation of laboratory-scale smoke data. Zinn *et al.*[4–6] have made detailed measurements of the physical characteristics of smoke particulates generated from various fuels in a combustion products test chamber. In addition to these basic studies, numerous smoke testing devices have been developed for categorizing the smoke-generation tendency of different material.[2] The most widely used is the National Bureau of Standards (NBS) smoke-density chamber,[7] in which the smoke characteristics of a material are represented by a specific optical density D_s[7] defined as

$$D_s = \frac{VD}{AL}, \qquad (1)$$

where V is the volume of the chamber; A is the surface area of the test sample; and L is the beam length through which the optical density D is measured. Seader *et al.*[2,8] have attempted to relate their theory to the NBS smoke chamber and to rank the smoke hazards of various fuels according to their measured D_s values. Robertson[9] also made predictions of the smoke characteristics of burning fuels in a fire from D_s measurements. Since correlation of the smoke characteristics in a real fire situation and in a laboratory test condition has not been fully demonstrated, and since current smoke data arise mainly from burning individual small samples at low surface heat flux, it is constructive to study the characteristics of smoke particles in a larger and more realistic fire.

In the present study, smoke particles generated from a wood fire in a ventilated model tunnel were examined. The model tunnel was set up such that the uniform arrangement of the wood lining on the tunnel walls and the single tunnel ventilation flow provided a convenient way of studying the generation of smoke particulates with respect to the wood burning process and to the development of the fire. The volume-to-surface mean diameter and mass concentration of the smoke particles, and the optical density and transmission of the tunnel exhaust gas were determined at the tunnel exit using an *in situ* optical device developed by Cashdollar *et al.*[10,11]. In addition, smoke particles were collected by a grid sampling technique, and their size and geometry were examined using transmission-electron-microscope photography. Smoke characteristics during the course of the fire are presented, and compared with studies from other investigators. Applicability of current smoke testing devices is also discussed based on the present measurements.

EXPERIMENTAL

The 0.3 m × 0.3 m × 10 m model fire tunnel shown in Figs. 1 and 2 was developed by Chaiken *et al.*[12–14] to study laboratory-scale tunnel fires and to model full-scale mine fires. As indicated in Fig. 2, numerous devices were employed for the measurement of flame-spread, temperature, pressure, heat flux, composition and flow of gases, and smoke particulates during the course of the fire. While measurement techniques have been reported elsewhere,[12] it is appropriate to mention here that gas composition (CO, H_2, CH_4, O_2 and CO_2) was determined by both batch samples analyzed by gas chromatography and automatic on-line analysis using non-dispersive infrared, thermoconductivity, and electrochemical techniques. In the present paper, only data relevant to smoke generation are reported. Results on other measurements are being reported elsewhere.[14]

A wood fire experiment using 3 cm thick and 7.0 m long virgin oak lining on the roof and two side walls of the tunnel was conducted (see Fig. 1). Before the experiment, the exhaust fan was set at a constant speed to

CCC-0308-0501/78/0002-0110 $03.50

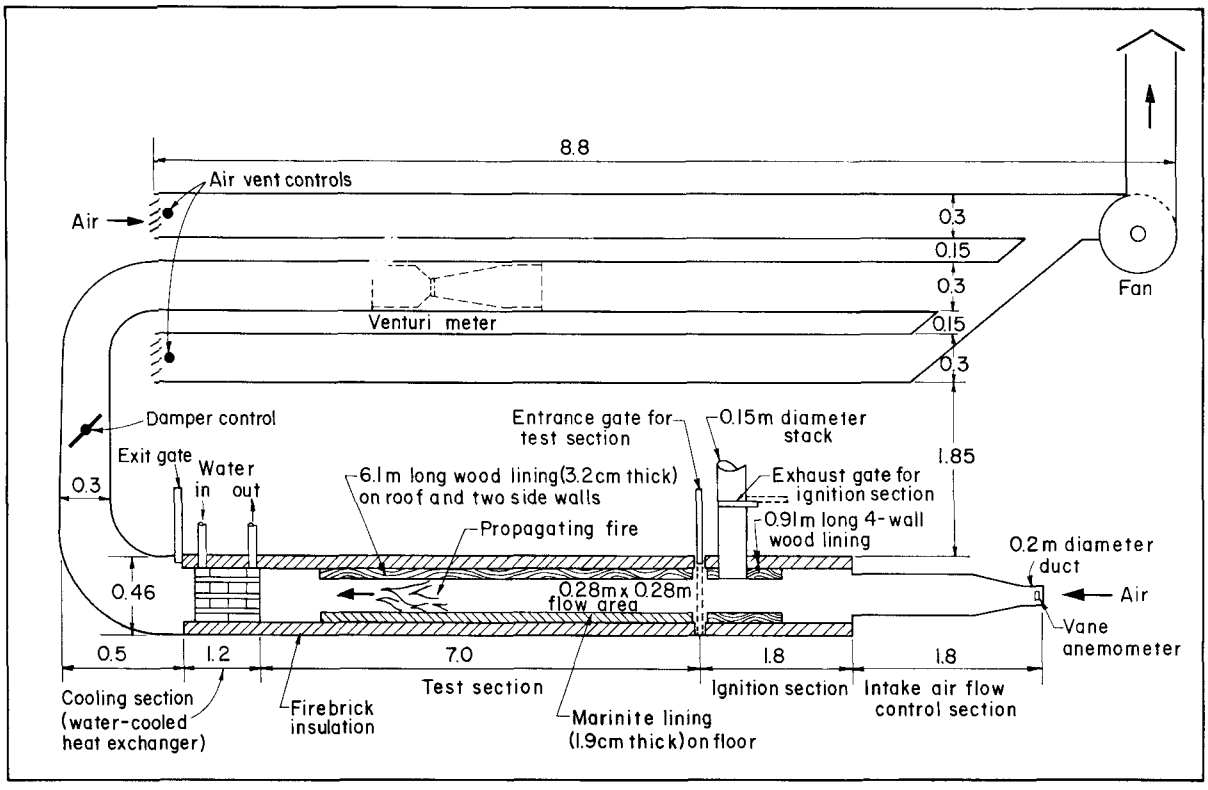

Figure 1. Vertical cross-section schematic of fire tunnel. All dimensions are in metres.

ventilate room air at a nominal velocity of 1.5 m s^{-1} through the tunnel, and the fan speed was kept constant during the test. The wood in the ignition section was first ignited by a premixed gas-burner. The gas-burner was immediately withdrawn from the tunnel when the flame started to spread downstream on the wood surface; subsequently, the entire wood lining became fully inflamed within 2 min. The fire was extinguished after 12 min by sealing and injection of nitrogen gas.

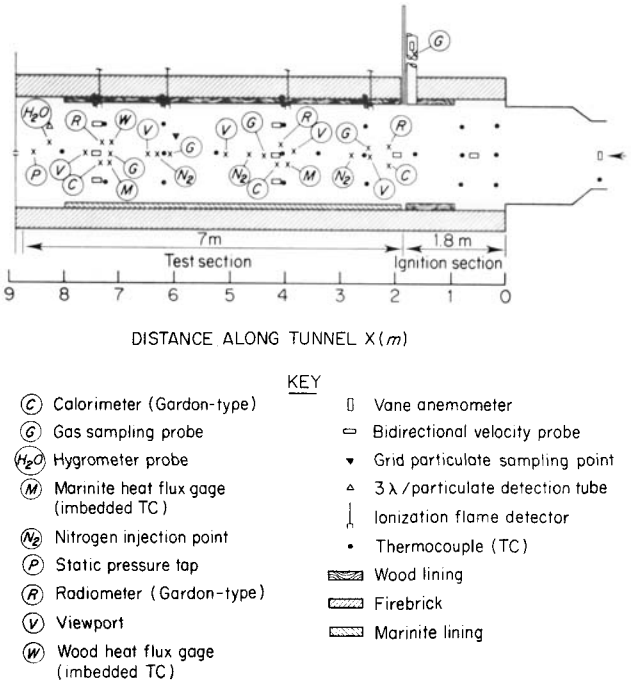

Figure 2. Instrumentation of fire tunnel (vertical cross-section).

The volume-to-surface mean diameter and mass concentration of the smoke particulates in the tunnel exhaust gas were determined at 7.2 m from the beginning of the wood lining (see Fig. 2) using optical transmission measurements through an 11 cm path length of the exhaust gas at three wavelengths of 0.45, 0.63 and 1.00 μm (first two are within visible spectrum). General description of this three wavelength (3λ) particulate detection technique was reported elsewhere.[10] Detailed description on the theory, design and testing of the technique is being reported.[11] Briefly, the technique involved theoretical calculation of the extinction efficiency K as a function of spherical particle diameter d, wavelength of the radiation λ, and complex refractive index of particles m from Mie single scattering theory, and experimental measurement of optical transmission at three wavelengths. Two refractive indices were used. The first was $m_1 = 1.8–0.6i$, which is an average of the index for carbon (1.95–0.66i) measured by Senftleben and Benedict[15] and the index for the soot particles from acetylene and propane flames determined by Dalzell and Sarofim.[16] The second was $m_2 = 1.8–0.3i$, which is similar to the index for soot (1.87–0.19i) used by Kunitomo and Sato[17] and the index for propane soot (1.9–0.35i) measured by Chippett and Gray.[18] The assumption of spherical particles appears to be reasonable as indicated by the transmission-electron-microscope photographs of the collected particles from the present fire experiment. The K values determined from Mie theory for single scattering are also valid for multiple scattering if the optical detector's angular field of view is sufficiently small to eliminate any significant amount of scattered radiation.[19] For a cloud of particles, the average extinction efficiency $\bar{K}(\bar{K} = \Sigma NKd^2 \Delta d / \Sigma Nd^2 \Delta d$, where N is the number of particles with diameter between d and $d + \Delta d$) was calculated as a

function of volume-to-surface mean diameter d_{32}($d_{32}=\Sigma Nd^3\Delta d/\Sigma Nd^2\Delta d$) using a log-normal size distribution with geometric standard deviation of 1.5 and 2.0. The log-normal distribution has been found to be applicable for smoke or soot particles by Chippett and Gray[18] and Foster.[20] From Bouguer's transmission law, the ratio of the logarithms of the measured transmissions at any two wavelengths is equal to the ratio of the computed $\bar{K}$ at the same wavelengths. Therefore, d_{32} of the smoke particles can be determined from the computed $\bar{K}$ ratios and the measured log-transmission ratios. To supplement the optical technique, smoke particles were collected on 3.2 mm diameter and 200 mesh stainless steel electron-microscope grids inserted into the tunnel at 4.9 m from the beginning of the wood lining. The collected smoke particles were then enlarged 50000 times in a photograph using transmission-electron-microscopy for size measurement.

RESULTS AND DISCUSSION

As mentioned earlier, the fire was permitted to take its own course under constant fan speed. Immediately following flame-spread on the wood surface, rapid evolution of volatile gas $\dot{m}_f$ from wood lining (at a surface heat-flux of about 1.6 cal cm^{-2} s^{-1}) partially displaced the ventilation air intake, causing a continuous decline (throttling) of the air supply $\dot{m}_a$ until steady burning was reached.[14] This fire throttling process is depicted in Fig. 3. It is estimated and also shown by the distribution of gas composition along the tunnel that the air supply $\dot{m}_a$ after throttling was sufficient for complete combustion of the volatile fuel gas from approximately the first 3 m of the wood lining; the remaining 4 m wood lining was mainly pyrolyzed to produce unburned volatile fuel. Therefore, subsequent to the decrease in $\dot{m}_a$, burning became extremely fuel-rich in the tunnel, which is reflected in the high CO and low O_2 concentrations of the tunnel exhaust gas, and the values of the normalized fuel/air ratio $R(R=4.6\ \dot{m}_f/\dot{m}_a$, where the constant 4.6 is the stoichiometric air/fuel ratio for wood combustion such that $R<1$ implies oxygen-rich burning and $R>1$ fuel-rich burning[21]) as shown in Fig. 4. The phenomenon of rapid transition from oxygen-rich to fuel-rich burning in tunnel wood fires was also observed by Roberts.[22]

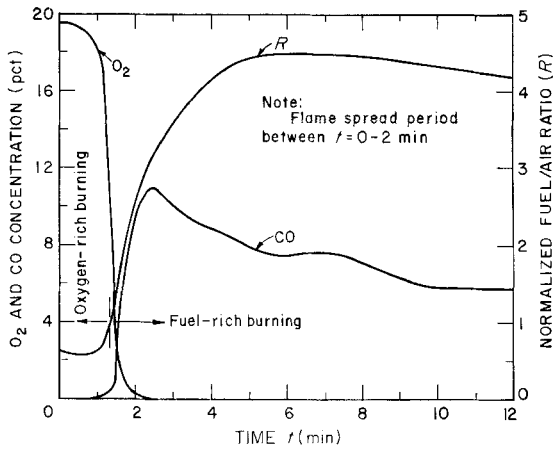

Figure 4. Variation of oxygen and carbon monoxide concentrations of tunnel exhaust gas and normalized fuel–air ratio during fire.

As fuel-rich burning proceeded, large quantities of smoke particulates were generated, resulting in a rapid decrease in the optical transmission of the exhaust gas as shown in Fig. 5. This rapid decrease in visibility coupled with the excess smoke particles and high temperature (~800°C) toxic gas CO represents an extremely hazardous situation in such a fire environment. Roberts[21, 22] previously noted the hazard associated with excess CO generated in a tunnel wood fire. The present work indicates that the hazard of excess smoke generation is also extremely severe as shown later in the paper.

From the transmission measurements τ at the three wavelengths during fuel-rich burning, the ratios of the logarithms of the transmission values were used to determine the volume-to-surface mean diameter d_{32} of the smoke particles. For either refractive index used in the calculations, the experimental data fit better to a log-normal distribution with standard deviation $\sigma_g=1.5$ than to one with $\sigma_g=2.0$. The data also fit better to the calculated $\bar{K}$ values for $m_2=1.8$–$0.3i$ than for $m_1=1.8$–$0.6i$, although the mean diameters calculated with either index agreed within the errors in the calculations. The best estimate of the mean particle size d_{32} was 0.13 ± 0.02 μm using m_2 and a log-normal size distribution with $\sigma_g=1.5$. The calculated extinction efficiency $\bar{K}$ at $\lambda=0.63$ μm was about 0.8 using m_1 and about 0.6

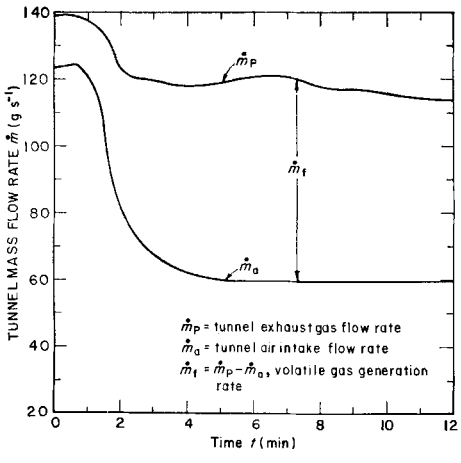

Figure 3. Tunnel mass flow rates during fire.

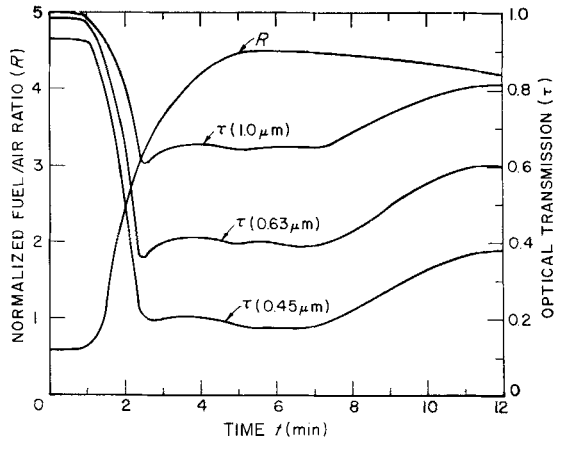

Figure 5. Variation of optical transmission through 11 cm thick tunnel exhaust gas during fire.

using m_2. For the transition and oxygen-rich burning periods, both the rapid change in the three transmissions with time and their small differences limited the accuracy of the calculation of d_{32} and $\bar{K}$. However, the average particle size was estimated to be about one-half as large as during fuel-rich burning.

A transmission-electron-microscope (TEM) photograph of some collected smoke particles during fuel-rich burning using the grid sampling technique is shown in Fig. 6. The individual particles are reasonably circular although some agglomeration occurred due to particle accumulation on the grid. The particle size and shape are somewhat typical of the other TEM photographs, where slightly larger particles are also noticed. Such spherical and distinctive particles in the present wood fire are in contrast to the irregular soot aggregates from propane flames shown by Chippett and Gray.[18] This could be due to the difference in fuels, and the present high temperature as compared with their low temperature environment at the smoke detection station. The diameter ($\sim$0.04–0.10 μm) of the particles in Fig. 6 is somewhat smaller than the 0.13 μm determined by the 3λ optical technique. This may be due to particle agglomeration from the grid sampling point to the 3λ optical station. Thus, in spite of the discrepancy, the 3λ particle detection technique gives reasonable particle size measurements.

The distinctive spherical smoke particles of average diameter $d_{32} \cong 0.1$ μm as determined from the present tunnel fire experiment are in agreement with the size measurement on the smoke particles generated from heating sawdust by Foster.[20] However, larger smoke particles of 0.2–1.2 μm average diameter from oxygen-rich flaming combustion of Douglas fir were measured by Bankston *et al.*[6, 23] Based on the present TEM photographs, it appears that some particle agglomeration is necessary to form such large particles. In addition, the present tunnel fire environment of high heat-flux and fuel-rich flaming combustion as compared with Bankston's low heat-flux oxygen-rich combustion could result in smoke particles with different characteristics. With respect to the values of 0.6–0.8 for the extinction efficiency $\bar{K}$, values of the same order were reported by Seader and Ou.[1]

From the measurement of d_{32} (taken to be 0.13 μm for the entire experiment) and τ, and using an average particle density ρ of 1.5 g per cm^3, the smoke particle

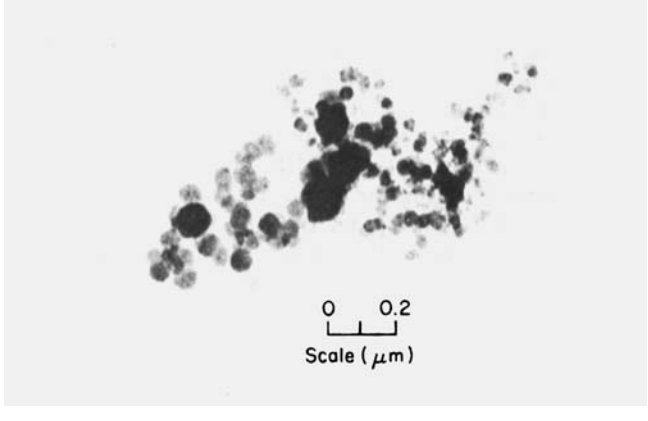

Figure 6. Transmission-electron-microscope photograph of smoke particles in tunnel fire.

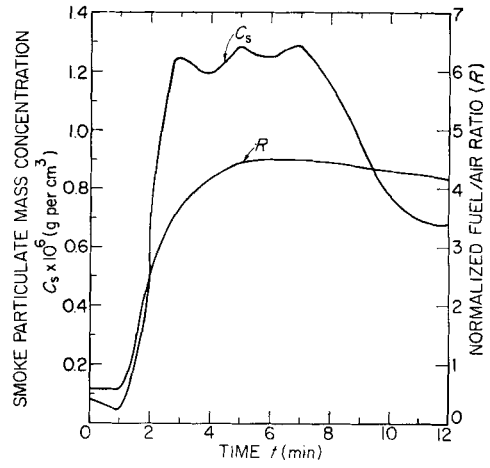

Figure 7. Variation of smoke mass concentration of tunnel exhaust gas during fire.

mass concentration C_s at the tunnel exit was calculated. Figure 7 shows that particle mass concentration increased from $\sim 7 \times 10^{-8}$ g cm^{-3} during oxygen-rich burning to $\sim 1.3 \times 10^{-6}$ g cm^{-3} during fuel-rich burning. This is apparently due to the decrease in air ventilation following fire throttling and the accumulation of the unburned smoke particles produced from wood pyrolysis during fuel-rich burning. Bankston *et al.*[6] reported lower C_s values of the order of 1×10^{-8} g cm^{-3} for flaming combustion of Douglas fir. Their lower particle mass concentrations were apparently due to the excess air dilution relative to the amount of wood burned, i.e. $R \ll 1$.

The smoke mass flow rate $\dot{m}_s$ calculated from the smoke mass concentration and the measured volumetric exhaust gas flow rate is plotted in Fig. 8. The volatile gas mass generation rate $\dot{m}_f$ and the CO mass flow rate $\dot{m}_{CO}$, calculated from Figs. 3 and 4, are also included in Fig. 8. It is noted that 0.08 wt% of the volatile gas $\dot{m}_f$ was converted to smoke particles $\dot{m}_s$ during the initial oxygen-rich burning period. The $\dot{m}_s/\dot{m}_f$ ratio then increased about ten-fold to 0.8 wt% during fuel-rich burning. The 0.8 wt% conversion compares favourably

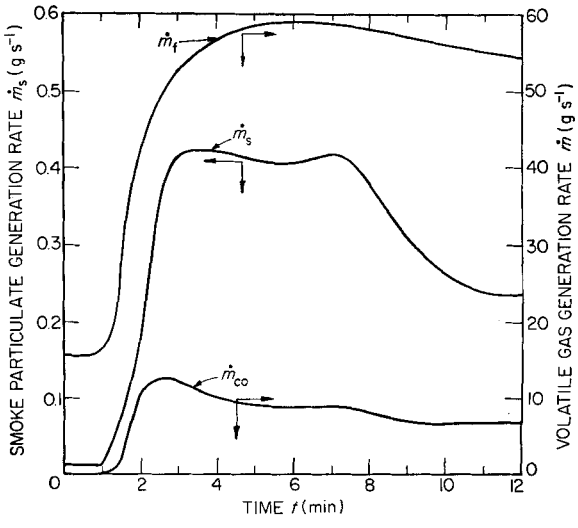

Figure 8. Variation of volatile, smoke and carbon monoxide mass flow rates during fire.

with the 1.0 wt%, reported by Cass.[24] The dependence of $\dot{m}_s/\dot{m}_f$ ratio on the burning mode is significant in terms of smoke hazard assessment of materials as most of the current smoke testing chambers operate in an oxygen-rich burning mode. Utilization of oxygen-rich burning smoke data in a real fire situation, which is often oxygen-deficient, could lead to serious problems. Generation of smoke particulates is seen to be parallel to CO production, with a maximum $\dot{m}_s/\dot{m}_{CO}$ ratio of about 4×10^{-5} during fuel-rich burning. The concurrent generation of excess smoke and CO in a real fire perhaps cause the simultaneous 'smoke inhalation' and 'CO poisoning'[25] that are often found in fire victims. Normalizing the generation rates of volatiles, CO, and smoke to the total burning wood surface area (51200 cm^2), their maximum mass generation rates per unit area during fuel-rich burning were 1.2×10^{-3} g cm^{-2} s^{-1}, 2.4×10^{-4} g cm^{-2} s^{-1} and 8.2×10^{-6} g cm^{-2} s^{-1}, respectively.

From Bouguer's law, the optical transmission τ of a light beam at wavelength λ through a gas of thickness L containing particles of mean diameter d_{32}, density ρ and mass concentration C_s is

$$\tau = \exp\left(-\frac{3\bar{K}LC_s}{2d_{32}\rho}\right), \quad (2)$$

where $\bar{K}$ is the average efficiency factor for both scattering and absorption. It can be readily shown that the optical density per unit length D/L is

$$D/L = 0.651\ \bar{K}\ C_s/(d_{32}\rho), \quad (3)$$

where D is the optical density defined as

$$D = -\log_{10}\tau. \quad (4)$$

As indicated in Eqn (3), the optical density per unit length is a function of the optical and physical properties $\bar{K}$, d_{32} and ρ of the smoke particulates, and the smoke mass concentration C_s. Seader *et al.*[3] defined the parameter $(D/L)/C_s$ as 'Particulate Optical Density (POD)', which has the advantage of being relatively constant for nonflaming (smoldering) and flaming combustion of hydrocarbon fuels. This is because $\bar{K}$ and d_{32} have different sets of values for the two modes of combustion. The particles for flaming combustion appear to be smaller and more light-absorbing than those produced in smoldering combustion. Average POD values of various fuels were found to be 19000 cm^2 g^{-1} for smoldering and 33000 cm^2 g^{-1} for flaming combustion by Seader *et al.*[3] Values of D/L at $\lambda = 0.63$ μm calculated from the corresponding τ measurement in Fig. 5 are plotted in Fig. 9 versus C_s as a function of time during the fire. The slope of the curves gives a POD value of 29000 cm^2 g^{-1}, which is close to Seader's 33000 cm^2 g^{-1} for flaming combustion. This is reasonable in view of the incomplete flaming combustion of the volatiles from the wood lining. Measurements of D/L and C_s from NBS smoke chamber for flaming combustion of oak[26] are also shown in Fig. 9 for comparison. Agreement is quite good in spite of the difference in the ventilated nature of the present tunnel and the sealed condition of the NBS chamber. Comparison between the two sets of data in Fig. 9 also suggests that initial burning of the oak sample in the NBS chamber was oxygen-rich; as combustion proceeds, more oxygen was consumed and more combustion products and smoke were produced,

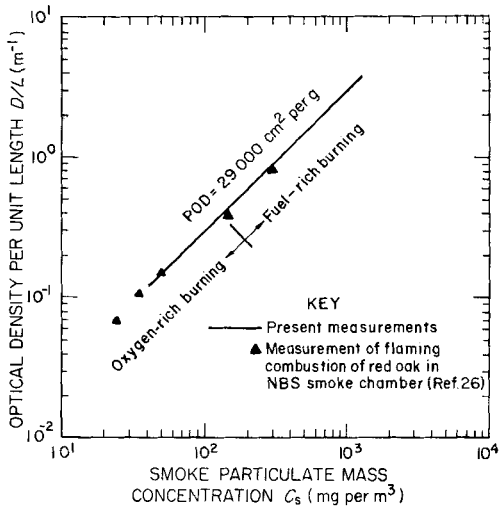

Figure 9. Variation of optical density per unit length of tunnel exhaust gas with respect to smoke mass concentration during fire.

leading to fuel-rich burning and a maximum value of D/L. Such a maximum D/L is still below the high D/L values measured in the present tunnel fire due to the high values of C_s in the tunnel exhaust gas. However, owing to the linear relationship between D/L and C_s, extrapolation of the NBS data into the fuel-rich zone falls in line with present measurements. On the other hand, the lower values of D/L and C_s reported by Bankston *et al.*[6, 23] fall in the lower left-hand corner of Fig. 9, representing a less hazardous fire situation than both the NBS and the present tests. A plot of D/L vs C_s such as Fig. 9 for a material is important because each set of D/L and C_s values is associated with certain visual obscuration and physiological hazards, which arise from certain fire environment. Perhaps smoke hazard ratings can be assigned to the sets of values of D/L and C_s to establish smoke hazard guidelines. Such guidelines would certainly have to come from more research work on the combined effect of D/L and C_s from smoke.

Visual obscuration by dense smoke clouds often causes panic and hysteria among people in a fire. In this connection, Silversides[27] has determined the visibility (maximum distance through which a person can see illuminated objects) as a function of optical density per unit length, D/L, for white light. His findings show that for a typical distance of 5 m, the corresponding threshold D/L value for visibility is 0.2 m^{-1}, and a 0.1 increase in D/L results in a reduction of visibility of about 3 m. It should be noted that these findings do not include the physiological effects of the irritants in the smoke on vision. In a real fire situation, the visibility as determined by Silversides would be substantially reduced by the irritants. Time variation of D/L obtained from the τ measurements during the fire is shown in Fig. 10. Values of D/L in the visible part of the spectrum (0.45 μm–0.63 μm) are greater than 2 m^{-1} for almost the entire burning period. For visible light at a central wavelength of 0.55 μm, D/L varies between 3 and 5 during fuel-rich burning, and the corresponding visibility would be less than 1 m, which is practically zero for any human escape or rescue measures. It might be mentioned also that in addition to smoke, condensation of the water vapor produced from a tunnel fire into an airborn mist far

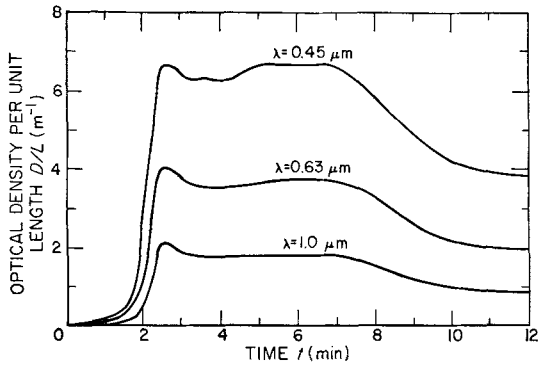

Figure 10. Variation of optical density per unit length of tunnel exhaust gas during fire.

downstream from the fire could also obscure visibility as shown by Heyn.[28]

As mentioned earlier, the parameter specific optical density $D_s = VD/(AL)$ has been used in interpreting NBS smoke chamber measurements for rating the smoke generation tendency of materials. Since the chamber is not vented during testing, D_s is calculated based on a resulting maximum D as smoke particles accumulate within the chamber. A better understanding of D_s can be obtained by replacing D with Eqn (2), such that

$$D_s = \left(\frac{V}{AL}\right)\left(\frac{3\bar{K}LC_s}{2d_{32}\rho}\right) \tag{5}$$

Since, for a given material at a fixed surface heat flux $\bar{K}$, d_{32} and ρ have different sets of relatively constant values for flaming and for smoldering combustion, D_s can be expressed as

$$D_s = b\frac{VC_s}{A} \tag{6}$$

where b is a constant equal to $3\bar{K}/2d_{32}\rho$ from Eqn (5). Since V and A are fixed as required by the test, or equivalently, the amount of material (fuel) and air (oxidizer) are fixed, C_s is expected to reach a constant (maximum) value, giving rise to a unique D_s for the material under test. Therefore, D_s is an indication of the amount of smoke generated per unit volume under the laboratory test conditions, but is not an intrinsic property of a material (see Seader *et al.*[2]).

Variables that may influence the value of D_s have been discussed by Seader *et al.*[2] One variable is air ventilation, an increase in which generally decreases D_s. The number of air changes, about 20 per min, for the present tunnel fire is significantly higher than the 20 air changes per hour used by Gaskill *et al.*[29, 30] in the NBS smoke chamber. If the volume enclosed by the wood lining in the present fire tunnel is taken as V, the wood lining surface area as A, and the beam length of the 3λ smoke detector as L, a maximum value of 0.17 is calculated for D_s for the present fire, whereas a value of 74 was reported by Hilado[31] for oak in the NBS smoke chamber without ventilation. Some estimates on the effect of ventilation on the D_s values in a NBS chamber have been made by Gaskill.[30] However, results are not yet conclusive. Uncertainties still exist (e.g. Robertson[9]) in applying the measured D_s values to a real fire situation. One can conceivably rank the smoke hazards of various materials under a single test condition according to their D_s values; however, different materials may have different end-use conditions that may give rise to drastically different potential fire environments, e.g. a ventilated underground mine fire as opposed to a free burning open fire. It appears that meaningful comparison of smoke hazard as well as other fire hazards of materials should be based on a set of test criteria that is realistically related to the end-use environment of the materials, instead of ranking all materials under a single set of test conditions.

As a final remark, it is of interest in the context of this paper to comment on the hazards due to smoke particulates and CO. Such comments are necessarily limited since the physiological and toxic effects produced by inhaled combustion products are still not well understood. Toxic levels for both short and long duration exposures are better known for CO than for smoke. Fassett and Irish[32] give empirical equations for time and CO concentration effects on toxic exposure. For example, 188 ppm (0.0188%) for an 8 h exposure is death threatening. For shorter duration of 5–30 min, 4000–10000 ppm (0.4–1.0%) of CO are shown to be fatal by Herpol *et al.*[33] As an approximation, the threshold concentration of 3.5 mg m^{-3} for 8 h exposure for carbon black[34] can be used to characterize the accumulative-type or long duration hazard of smoke as opposed to a more immediare-type hazard. The severe physiological hazards of the CO and smoke concentration levels of the present tunnel wood fire (Figs. 4 and 7) become obvious when compared with the above threshold values. It will be extremely difficult to dilute the present high concentration of smoke and CO to acceptable levels by air flow in a typical mine ventilation system. For example, a 500-fold air dilution is required to bring the 10% CO (see Fig. 4) to a level of 188 ppm and a 2900-fold dilution is necessary to reduce the 10^3 mg m^{-3} smoke particle concentration (see Fig. 8) to a level of 3.5 mg m^{-3}.

CONCLUSION

The smoke hazards of a laboratory-scale tunnel fire in terms of smoke mass concentration and optical transmission are demonstrated by the present investigation. It is not unreasonable to expect such hazards in a full-scale mine timber fire as fuel-rich burning was demonstrated by Roberts[21] in some large-scale mine timber fires. The present study shows that smoke generation in a tunnel fire is strongly coupled to ventilation air flow and fuel gas generation. Such important factors are apparently still difficult to simulate in current smoke testing apparatus. The exceedingly high concentrations of smoke and CO generated in a tunnel fire suggests stringent fire testing for materials used in a tunnel configuration. Therefore, realistic comparison in smoke hazards as well as other fire hazards of materials should be based on a set of test criteria that is realistically related to their end-use conditions and potential fire environments.

Acknowledgement

The authors are thankful to C. Bennett, L. Dalverny, A. Damick, R. Diehl, F. Donnelly, W. Hoffman, M. Harris and J. Opferman of PMSRC for their experimental assistance.

REFERENCES

1. J. D. Seader and S. S. Ou, *Fire Res.* **1**, 3 (1977).
2. J. D. Seader and I. N. Einhorn, Some Physical, Chemical, Toxicological and Physiological Aspects of Fire Smokes, *Sixteenth Symposium (International) on Combustion*, p. 1423. The Combustion Institute, Pittsburg, Pennsylvania (1977).
3. J. D. Seader and W. P. Chien, *J. Fire Flammability* **6**, 294 (1974).
4. B. J. Zinn, E. A. Powell, R. A. Cassanova and C. P. Bankston, *Fire Res.* **1**, 23 (1977).
5. C. P. Bankston, R. A. Cassanova, E. A. Powell and B. J. Zinn, *J. Fire Flammability* **7**, 165 (1976).
6. C. P. Bankston, E. A. Powell, R. A. Cassanova and B. J. Zinn, *J. Fire Flammability* **8**, 395 (1977).
7. D. Gross, J. J. Loftus and A. F. Robertson, Methods for Measuring Smoke from Burning Materials, Symposium on Fire Test Methods—Restraint and Smoke (1966), ASTM STP 422, P. 166. American Society for Testing and Materials, Philadelphia, (1967).
8. W. P. Chien and J. D. Seader, *Fire Technol.* **11**, 206 (1975).
9. A. F. Robertson, *Fire Technol.* **11**, 80 (1975).
10. K. L. Cashdollar, C. K. Lee and J. M. Singer, Smoke Particle Size and Concentration Measurement by a Three-Wavelength Light Transmission Technique, presented at the 1977 Eastern States Fall Technical Meeting, The Combustion Institute, Hartford, Connecticut (1977).
11. K. L. Cashdollar, C. K. Lee and J. M. Singer, A Three-Wavelength Light Transmission Technique for Measuring Smoke Particle Sizes and Concentrations, in preparation.
12. R. F. Chaikem, C. K. Lee and J. M. Singer, *Model Coal Tunnel Fires in Ventilation Flow*. US Bureau of Mines Report of Investigations, in press.
13. C. K. Lee, R. F. Chaiken and J. M. Singer, *Wood Precharring: A Novel Fire-Retardancy Technique*. US Bureau of Mines Report of Investigations, No. 8299 (1978).
14. C. K. Lee, R. F. Chaiken and J. M. Singer, *Model Tunnel Wood Fires in Ventilation Flow*. US Bureau of Mines Report of Investigations, in preparation.
15. H. Senftleben and E. Benedict, *Ann. Phys. (Leipzig)*, **54**, 65 (1918).
16. W. H. Dalzell and A. F. Sarofim, *J. Heat Transfer, Trans. ASME* **91**, 100 (1969).
17. T. Kunitomo and T. Sato, *Bull. JSME* **14**, (67) 58 (1971).
18. S. Chippett and W. A. Gray, *Combust. Flame*, **31**, 149 (1978).
19. J. R. Hodkinson, The Optical Measurement of Aerosols, in *Aerosol Science*, ed. by C. N. Davies, Chapt. X. Academic Press, New York (1966).
20. W. W. Foster, The Size of Wood Smoke Particles, in *Aerodynamic Capture of Particles*, ed. by E. G. Richardson. Proceedings of a Conference Held at B.C.U.R.A., Leatherhead, Surrey, England (1960), Pergamon Press, New York (1960).
21. A. F. Roberts, *Combust. Flame* **11**, 365 (1967).
22. A. F. Roberts, *Min. Eng.* 699 (September 1969).
23. E. A. Powell, C. P. Bankston, R. A. Cassanova and B. J. Zinn, Effect of Environmental Temperature Upon the Physical Characteristics of the Smoke Produced by Burning Wood and PVC Samples, presented at the 1977 Eastern States Fall Technical Meeting, The Combustion Institute, Hartford, Connecticut (1977).
24. R. A. Cass, *J. Cell. Plast.* **3**, (1) 41 (January 1967).
25. B. A. Zikria, D. C. Budd, H. F. Floch and J. M. Ferrer, *A Clinical View of 'Smoke Poisoning'*. Proceedings of International Symposium on Physiological and Toxicological Aspects of Combustion Products, University of Utah, Utah, 1974, p. 47. National Academy of Science, Washington, DC (1976).
26. T. Y. King, *J. Fire Flammability* **6**, 222 (1975).
27. R. G. Silversides, Measurement and Control of Smoke in Building Fires, Symposium on Fire Test Methods—Restraint and Smoke (1966), ASTM STP 422, p. 125. American Society for Testing and Materials, Philadelphia (1967).
28. W. Heyn, Underground Measurement of Smoke Density at the Tremonia Experimental Mine in Order to Determine Visibility in Fire Gases, presented at the 17th International Conference of Directors of Safety in Mines Research, Varna, Bulgaria (1977).
29. J. R. Gaskill, *J. Fire Flammability* **1**, 183 (1970).
30. J. R. Gaskill, R. D. Taylor, H. W. Ford and H. H. Miller, *J. Fire Flammability* **8**, 166 (1977).
31. C. J. Hilado, *Flammability Handbook for Plastics*, p. 42. Technomic, Stamford, Connecticut (1969).
32. D. W. Fassett and D. C. Irish, *Industrial Hygiene and Toxicology*, Vol. II, 2nd Revised Edn, p. 930. *Interscience Publishers, New York*. (1963).
33. C. Herpol, R. Minne and E. Van Outryve, *Combust. Sci. Technol.* **12**, (4, 5 and 6) 217 (1976).
34. J. A. Danielson, *Air Pollution Engineering Manual*, p. 877. National Center for Air Pollution Control, Cincinnati, Ohio (1967).

Received 21 February 1978